

Phobos Encounter Trajectory and Maneuver Design

R.E. Diehl,* M.J. Adams,† and E.A. Rinderle Jr.‡
Jet Propulsion Laboratory, Pasadena, Calif.

In February 1977, the Viking 1 Orbiter made repeated flybys of the Martian satellite Phobos at distances near 100 km. These close encounters allowed a detailed scientific investigation of the nature and origin of Phobos. A sequence of three maneuvers was required to achieve the encounters. This paper presents the trajectory analysis performed to accommodate the scientific objectives and the spacecraft propulsive maneuver strategy used to achieve the desired trajectory while satisfying operational constraints. The actual maneuvers executed and the resultant Phobos encounter conditions are presented.

I. Introduction

IN 1971, Mariner 9 took the first closeup pictures of the Martian satellite Phobos. These pictures, taken from distances as close as 5500 km, showed Phobos to be a very irregular, heavily cratered body.¹ The first photograph of Phobos taken by the Viking 1 Orbiter (V01) in July 1976 showed regions not viewed by Mariner 9 also to be heavily cratered. In September 1976 the Viking 2 Orbiter (V02) came within 900 km of Phobos. A spectacular photograph showed Phobos to be marked by striations and chains of small craters. These features puzzled scientists and pointed to the need for additional high-resolution coverage.

Another reason for additional study of Phobos is the question of its origin. Is Phobos a captured asteroid or was its formation due to a condensation process? Encounters with Phobos at distances much closer than the Mariner 9 encounters would provide new data required to help confirm or reject current theories.

In February 1977 the opportunity existed for V01 to make repeated flybys of Phobos at distances on the order of 100 km. Preliminary studies had shown that these encounters were obtainable with only small changes to the V01 orbit.² The trajectory and maneuver design required to obtain the encounters presented an exciting challenge, since multiple close satellite encounters at this distance had not been attempted before.

The primary scientific objectives of the Phobos encounter mission were to determine the mass and volume of Phobos and to obtain high-resolution imaging and infrared coverage of the surface. In order to design an encounter mission that would enable the satisfaction of the scientific objectives, the spacecraft trajectory was targeted to give 10 encounters within 150 km on the illuminated side of Phobos. In addition, at least one approach within 70 km was desired.

For V01 to have a close encounter with Phobos, two conditions must be satisfied. First, their orbits must nearly intersect. Second, the passages of Phobos and V01 through the line of nodes (the intersection of their orbital planes) must occur at nearly the same time. Sections II and III describe the geometry needed to satisfy the first condition; Sec. VII presents the strategy necessary to satisfy the second requirement.

II. Phobos Encounter Geometry

Figure 1 shows the February 1977 encounter geometry at the instant of orbit intersection between Phobos and V01 in a view from near the Martian North Pole. The nearly circular orbit of Phobos has a radius of approximately 9380 km and an inclination of about 1 deg. The eccentricity and inclination of the V01 orbit were about 0.75 and 39 deg respectively. The V01 periapsis altitude was approximately 1500 km with the subperiapsis point in the northern hemisphere.

Figure 1 shows that an orbit intersection occurs along the line of nodes at the descending crossing. Therefore, for an encounter at this crossing, the spacecraft must approach Phobos from above the Phobos orbit plane. At the ascending node, the V01 orbit intersects the line of nodes inside the orbit of Phobos. The precession of the line of apsides due to the oblateness of Mars causes the V01 descending node intersection to move radially inward towards Mars. At the same time, the ascending node intersection moves radially outward. Let ΔR be defined as the distance between the V01 and Phobos orbit along the line of nodes. The quantity ΔR is considered positive when the spacecraft orbit intersects the lines of nodes outside the orbit of Phobos. Therefore, for this descending node crossing, ΔR changes with time from a positive quantity to a negative quantity. The V01 orbit geometry required for intersection ($\Delta R = 0$) occurs naturally due to the rotation of the line of apsides.

A natural intersection would have occurred at the descending node on February 9. However, due to the timing between Phobos and the Orbiter a close encounter did not exist. Therefore, it was necessary to use propulsive maneuvers to change the spacecraft orbital period to produce an encounter mission. Also, mission operations found it desirable to delay the orbit intersection by approximately two weeks. Therefore it was necessary to correct two spacecraft orbital elements, the argument of the periapsis and periapsis altitude, to delay the encounter.

III. Trajectory Strategy

The conic equation

$$r = \frac{a(1-e^2)}{1+e \cos \eta} \quad (1)$$

where r is the Mars-to-spacecraft radial distance, a is the spacecraft semimajor axis, e is the eccentricity and η is the true anomaly can be used to calculate the approximate value of the argument of periapsis, ω , required for orbit intersection. Since Phobos has a small inclination, the spacecraft will intercept it when $\eta \approx -\omega$ (ascending node) and when $\eta \approx 180 \text{ deg} - \omega$ (descending node). Assuming that Phobos is in an exactly circular orbit, there will be an intersection with the V01 orbit when r equals the semimajor axis of Phobos. Let a^* be the semimajor axis of Phobos. The

Presented as Paper 78-49 at the AIAA 16th Aerospace Sciences Meeting, Huntsville, Ala., Jan. 16-18, 1978; submitted March 13, 1978; revision received May 26, 1978. Copyright © American Institute of Aeronautics and Astronautics, Inc., 1978. All rights reserved.

Index category: Spacecraft Navigation, Guidance, and Flight-Path Control.

*Senior Engineer, Systems Division,

†Engineer, Systems Division.

‡Senior Computing Analyst, Systems Division.

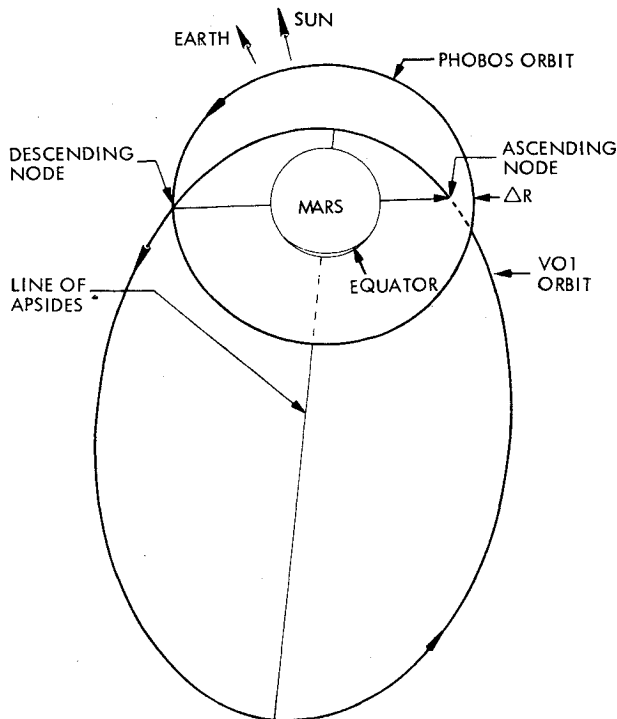


Fig. 1 Phobos encounter geometry.

evaluation of Eq. (1) at the descending node yields

$$\omega = \cos^{-1} \left(\frac{1}{e} - \frac{a(1-e^2)}{a^*e} \right) \quad (2)$$

To insure multiple close encounters, the spacecraft semimajor axis is fixed. (Details will be discussed later.) The spacecraft periaxis radius r_p can be expressed as $r_p = a(1-e)$. Substituting this expression for r_p into Eq. (2) yields

$$\omega = \cos^{-1} \left(\frac{r_p^2 - 2ar_p + a^*a}{a^*(a-r_p)} \right) \quad (3)$$

Equation (3) shows that for a fixed value of a , ω and r_p are the orbit parameters that control ΔR . Figure 2 represents the constraint curve defined by Eq. (3) which gives a zero value for ΔR for the descending node encounter pictured in Fig. 1. The V01 periaxis altitude h_p (a key planetary quarantine parameter) is plotted instead of periaxis radius. For an intersection of the orbits of the spacecraft and Phobos to occur on a specified date, ω and h_p must satisfy the constraint given in Fig. 2 at the specific time. Propulsive maneuvers can be used to alter the date of orbit intersection by changing ω and h_p . To cause the orbit intersection to occur on a given date with a specific h_p , ω should be adjusted so that orbit precession between the maneuver epoch and desired intersection epoch will allow ω to reach the value required for orbit intersection. For the V01 orbit, ω precessed at the rate of about 0.17 deg/day. Therefore, to change the intersection date by 10 days while keeping h_p fixed, a maneuver which changed ω by 1.7 deg would be required.

The ω precession rate maps into a ΔR rate of about -23 km/rev at the descending node. Therefore, with proper phasing, several relatively close encounters on either side of the $\Delta R = 0$ date were possible. To obtain a close encounter on each revolution, the orbital periods of the spacecraft and Phobos must have an $n:1$ commensurability where n is an integer. A period as close as possible to the pre-Phobos encounter period (24.6 h) was desired to minimize both the maneuver propellant requirements and the impact on the other Orbiter science experiments. Since the orbital period of

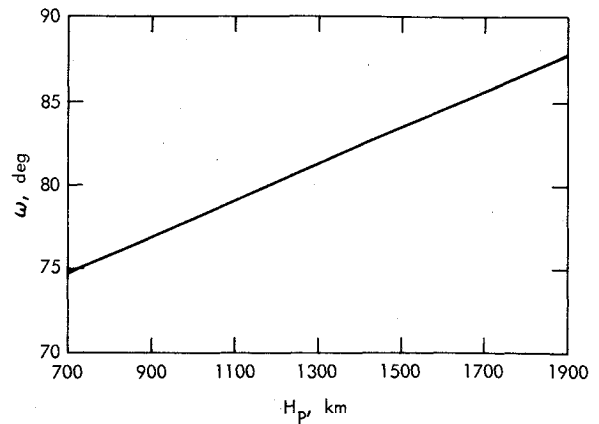
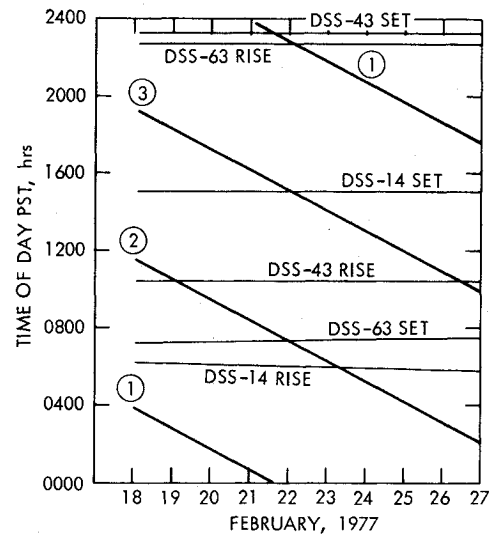
Fig. 2 Constraint curve for $\Delta R = 0$.

Fig. 3 Tracking station view periods.

Phobos is 7.65 h, a spacecraft period slightly less than 23 h is in a 3:1 commensurability with Phobos. This period was selected for the Phobos encounter mission. A 2:1 commensurate period would have given more encounters (one every 15.3 h), but would have required additional propellant and would have been too taxing to mission operations.

Once the orbit intersection date and V01 period have been chosen, the spacecraft must be phased with Phobos so that there is a nearly simultaneous arrival at the line of nodes. Due to its orbital period, Phobos passes through the descending node three times every 23 h. Once the spacecraft is phased for a specific encounter on the first day of the encounter period, the remaining encounter times are defined.

The selection of the first encounter opportunity was based on several factors. The primary consideration was navigation, which is discussed later in this paper. A secondary consideration was the tracking station view periods for each of the encounter sequences. Figure 3 presents the rise and set times for stations 14 (Goldstone, Calif.), 43 (Bellima, Australia), and 63 (Robledo, Spain) for late February 1977. The encounter times for the three sequences were determined from the epoch of Phobos passage through the line of nodes. The encounter sequence labeled three, the one chosen for the Phobos encounter mission, gave the most favorable station coverage. It was the only sequence that gave continuous coverage from a single station over the entire encounter period. Such coverage was not necessary, but was considered desirable for reliability reasons. Another favorable aspect of this sequence was that it gave encounter times between 10 a.m. and 7 p.m. PST.

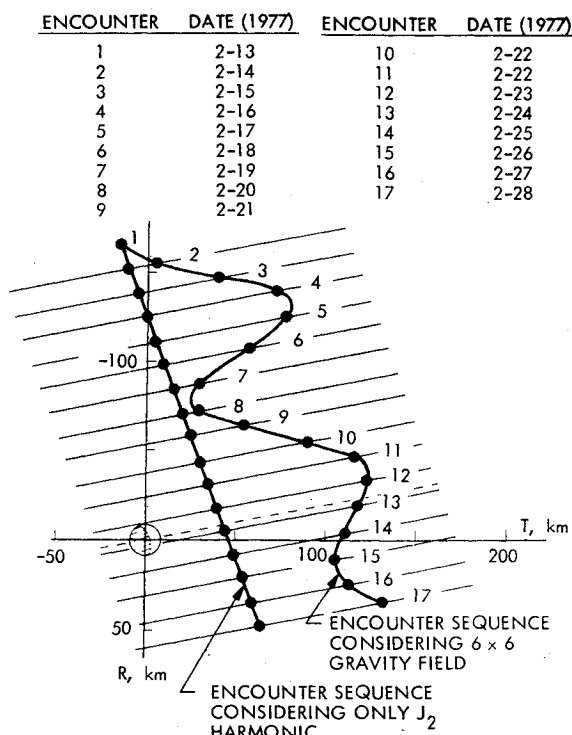


Fig. 4 Tesserall harmonic effects on Phobos encounters.

IV. Targeting Strategy

The flyby geometries for the encounter period are shown in Fig. 4 for a typical targeted trajectory considering a sixth degree and order gravity model. The R and T axes form an encounter plane which is perpendicular to the incoming asymptote to Phobos. The T axis is parallel to the Mars equatorial plane and is perpendicular to the R axis. The direction to Mars is 63 deg below T and 50 deg out of the figure, while the direction to the sun is 16 deg above T and 37 deg into the paper. The location of the terminator on Phobos at encounter is shown. The dots above and to the right of Phobos indicate the points of closest approach for each encounter during the encounter period. Perturbations of the Mars gravity field on the spacecraft orbital elements determine the positional behavior of the dots. Each of the encounters is numbered and a table is given with the corresponding encounter date.

The parallel lines shown passing through each dot represent contours of constant ω . Each line is the locus of possible encounters for a specified encounter date considering only small changes to the spacecraft orbital period. Adjustment of the spacecraft period before the first encounter will cause all the encounter positions to move in the R - T plane along the ω line corresponding to that encounter date. The encounter position change is due to an accumulated timing change between the spacecraft and Phobos over the revolutions between the period change and the specific encounter. Precession of ω causes the encounters to fall on subsequent lines. The dashed line corresponds to the ω line passing through the center of Phobos ($\Delta R = 0$). For this particular orbit geometry, an increase in the spacecraft orbital period will cause the encounter location to move in the positive T direction.

As shown in Fig. 4, a contour connecting the encounter points will be a straight line if only the J_2 harmonic is considered for the Mars gravity field. When a higher order gravity field is considered, the contour is not a straight line, since the tesserall harmonics will cause periodic oscillations in the spacecraft orbital period. If all values of the oscillating period are greater than the 3:1 Phobos commensurate period, each successive encounter point will move in the positive T direction. If all values are less, each successive encounter

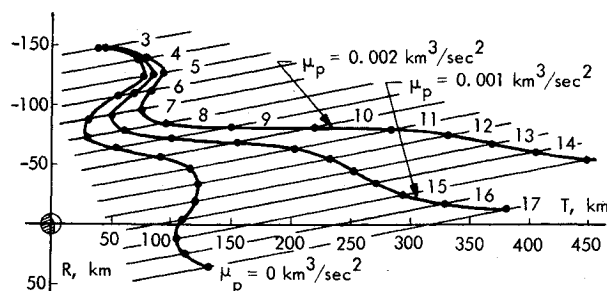


Fig. 5 Phobos mass effects on Phobos encounters.

point will move in the negative T direction. Period oscillations about the Phobos commensurate period alternately move the encounter points in a positive or negative T direction.

The encounter locations can be displaced in a direction perpendicular to the ω lines by changing the initial value of ω . For each +0.17 deg change in ω , the encounter date for a specific ω line will decrease by 23 h, since one less revolution of precession is needed for ω to reach the value required by the ω line. Similarly, for each -0.17 deg change in ω the encounter date will increase by 23 h. Changes which are not integer multiples of 0.17 deg cause the encounter locations to lie on ω lines between the ω lines shown in Fig. 4. Therefore, it is possible to target to a spacecraft orbital period and ω , such that any single encounter occurs at an exact point in the R - T plane. Once this encounter is targeted, all of the other encounter locations are determined by the oscillating period and ω precession.

V. Phobos Mass Effects

In Fig. 4 the encounters do not reflect the perturbations to the spacecraft orbit due to the mass of Phobos. In Fig. 5 the same encounter sequence is presented including Phobos mass effects for gravitational constants of Phobos equal to 0.002 and 0.001 km^3/s^2 . In this range of masses for Phobos, the perturbations to the spacecraft significantly affect only the orbital period. Therefore, encounters of the same date lie on the same ω line. The effect of increasing the Phobos mass for this orbit geometry is to increase the period causing subsequent encounters to have larger closest approach distances.

Figure 5 shows that the first several encounters are not greatly displaced from each other. However, after the closest encounters, the displacement between the encounter sequences grows rapidly as timing errors grow due to accumulated period differences over the previous revolutions. Therefore a conservative trajectory targeting strategy would assume a zero mass for Phobos. For if too large a value had been used in the targeting strategy, the actual resulting encounters would have moved in a negative T direction allowing the possibility of an impact trajectory.

VI. Maneuver Objectives

The goal of the maneuver strategy was to achieve the desired Phobos encounter trajectory with precise navigation accuracy in the presence of many spacecraft and operational constraints, including: 1) available propellant, 2) Planetary Quarantine (PQ) requirements, 3) spacecraft communications and performance limitations, 4) minimum operational lead time between maneuvers, and 5) lander-orbiter telemetry relay requirements.

The trajectory objectives placed a number of interesting and stringent requirements on the control of the spacecraft orbit. The nominal minimum closest approach of 70 km, coupled with the requirement of ten or more sequential encounters, levied very strict constraints on orbital period control. Delaying the natural $\Delta R = 0$ date created additional complications in reorienting the spacecraft orbit. Mission objectives included efficient propellant use, operational flexibility, and a negligible Phobos impact probability.

The primary maneuver problem is to satisfy the trajectory and mission objectives while coping with orbit determination and maneuver execution errors. These design considerations evolved into a sequence of three maneuvers which insured a precise, reliable spacecraft delivery.

VII. Maneuver Strategy

Two key design considerations formed the basic outline of the strategy. First, the spacecraft revolutions in which maneuvers could be performed were specified primarily by operational considerations. Second, the nominal strategy could employ, at most, three propulsive maneuvers. (A fourth maneuver was developed as an impact avoidance contingency.) If actual postmaneuver trajectory information were to be included in the first Phobos observations on February 18, operational development time precluded performing a maneuver after February 11. This development time consisted of 24 h of radiometric tracking, 2 days for orbit redetermination, 2 days for the science sequence design and verification, and 2 days for generation and transmission of spacecraft commands. Navigation considerations favor minimizing the time between the final maneuver and the encounter sequence to reduce the propagation of execution and prediction errors (especially period errors that accumulate each revolution into the final encounter timing error). Therefore February 11, was selected as the date for the last maneuver. Similarly, the last maneuver in the sequence must rely on the knowledge of the actual performance of the previous maneuver. Again, the need to reduce the time for errors to propagate was overruled by the minimum operational lead time. Consequently, the second maneuver was performed on February 4. Previously committed mission resources plus minimum development time restricted the first maneuver to the time span between January 20 and 28. The first maneuver execution was finally selected, as discussed later, for January 22.

Two maneuver guidelines assured satisfaction of the restrictions in the number of maneuvers and propellant allocation. The first guideline employs progressively smaller maneuvers, each correcting the errors in the previous maneuver. The second guideline is to plan a nominal (error free) maneuver sequence that would utilize only two maneuvers to effect the desired encounter conditions. The third maneuver is required statistically, but only to remove any residual errors.

Careful consideration of the fixed maneuver dates, maneuver guidelines, and actual maneuver targets determined the primary function of each nominal maneuver. The first maneuver was required to initiate the time "phasing" period needed to intercept Phobos at the next maneuver opportunity. The second maneuver then "synchronizes" with the 3:1 Phobos commensurate period and maintains relatively close encounters each Orbiter revolution. These two roles, phasing and syncing, are fundamental functions in effecting the required timing condition. In light of execution and prediction errors, the second maneuver will actually phase to the final maneuver which will then "nearly" synchronize to Phobos.

These timing concepts are conveniently visualized in terms of "timing offset." Timing offset (ΔT) is the time required for Phobos to reach the line of nodes after the Orbiter passes through it on a specified Orbiter revolution. (Note that the necessary and sufficient conditions for impact are $\Delta T \approx 0$ and $\Delta R \approx 0$.) For example, on January 22 the Orbiter passes through the descending line of nodes at $\approx 7:24$ UTC. During this revolution Phobos passed through the line of nodes at $\approx 1:00$, $9:00$, and $17:00$, giving a timing offset for each encounter opportunity of -6.4 , $+1.6$, and $+9.6$ h, respectively. (Convention usually defines $-\frac{1}{2}P < \Delta T \leq \frac{1}{2}P$ where P is the Orbiter period.) A $\Delta T = +1.6$ h on January 22 indicates that the Orbiter passed through the line of nodes 1.6 h before Phobos. Although timing offset gives time phasing in-

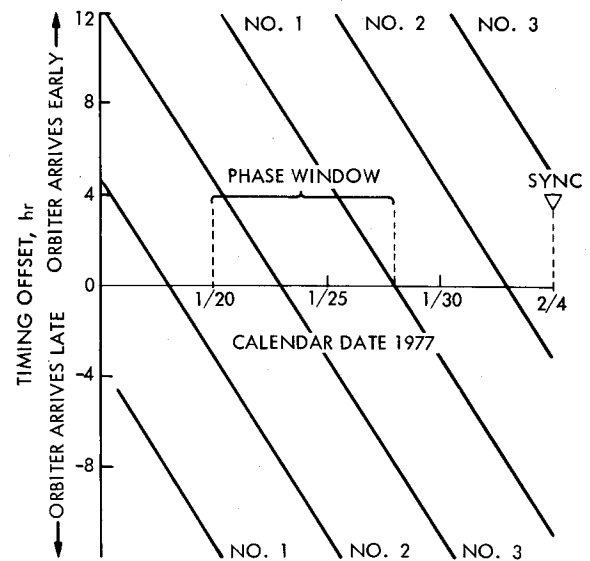


Fig. 6 Timing diagram.

formation only at specified event times, an array of such offsets can be plotted to reveal additional information.

The slope of the timing diagram line reflects the Orbiter period. A horizontal timing line represents the 22.95 h Phobos commensurate period to be achieved by the Orbiter. The negatively sloped lines in Fig. 6 display the 24.6 h Orbiter period before January 22. The labels correspond to the three encounter opportunities that existed on each Orbiter revolution. The change in slope from these lines to a zero slope corresponds to the total -1.65 hr period correction required to synchronize.

The selected strategy, consistent with the established propulsive maneuver guidelines, was to produce a substantial portion of the total period change with the first maneuver. This strategy is equivalent to locating the revolution of the phase maneuver near an abscissa intercept on the timing diagram. That is, the phase maneuver is executed on a revolution in which the Orbiter and Phobos line-of-nodes passages are nearly time coincident ($\Delta T \approx 0$). Also if the initial period is greater than the final period, it is propellant inefficient to phase to a particular Phobos nodal crossing from an Orbiter revolution which has a negative timing offset. Phasing from a negative ΔT requires a period less than 22.95 h, i.e., a positive-sloped timing offset behavior. Phasing from a positive ΔT , involves interim periods that will always be bracketed by the initial and final periods. This phasing constraint insures that orbital energy is always removed.

These considerations effectively ruled out the No. 2 encounter sequence, since the abscissa intercepts occur outside the permissible phase window. From a navigation point of view, the remaining two opportunities were equally obtainable. The No. 3 sequence provided better spacecraft tracking conditions during the encounter and was finally selected. January 23 provided an ideal intercept; however, it conflicted with a previously scheduled Orbiter science event. January 22 was finally selected for the phase maneuver. Figure 7 shows the nominal timing strategy.

The period change required for the first maneuver may now be determined by connecting the timing offset on January 22 to a zero ΔT on February 4. The resultant period and period change are 23.046 and -1.58 h, respectively. The nominal period change for the second maneuver becomes -0.07 h.

The approximate in-orbit location (true anomaly) of these maneuvers is a compromise between propellant usage and orbit control. The large period correction associated with the phase maneuver must be done near periapsis where the period change capability is high. Conversely, the sync maneuver should be placed near apoapsis where the period sensitivity is

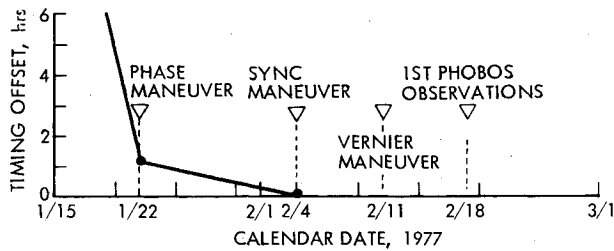


Fig. 7 Nominal timing diagram.

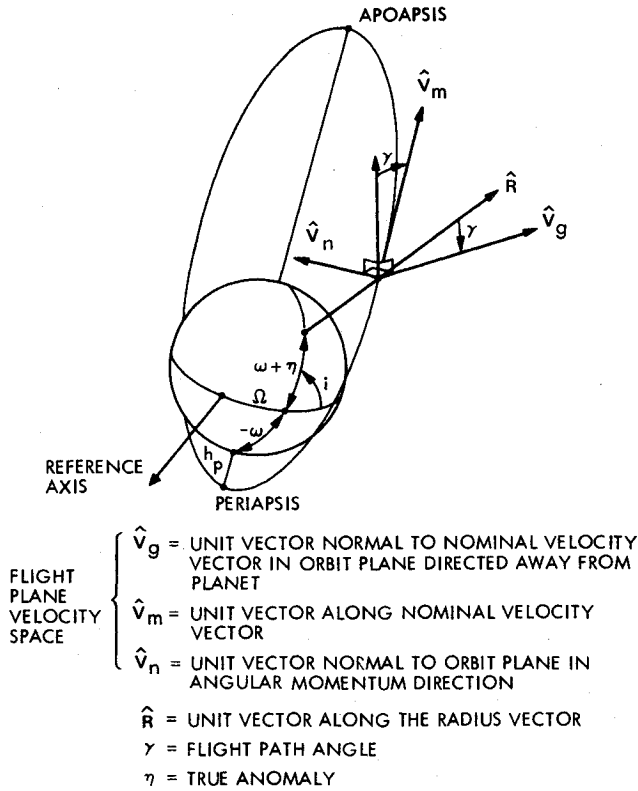


Fig. 8 Flight plane velocity space.

low and period errors are minimal. The same argument applies to placing the third maneuver near apoapsis. These assumptions in true anomaly vs control were valid for this maneuver sequence since the proportional errors could be neglected.

This preliminary timing strategy provided a framework which significantly reduced the complexities involved in implementing the required geometry condition. Incorporating the corrections in ω and h_p was the final step in defining the maneuver functions.

Delaying the $\Delta R = 0$ date with the Orbiter eccentricity would require increasing h_p . However, the project wanted to reduce h_p after the Phobos sequence. Effecting the correct geometry for $\Delta R = 0$ on February 25 would rely on correcting ω , i.e., an in-plane rotation of the orbit plane about the angular momentum vector. The previously stated maneuver guidelines and careful consideration of the physical problem resulted in the decision to implement most of the ω correction along with the large period correction. A small in-plane rotation of -0.55 deg by the nominal sync maneuver was unavoidable. The total change in ω to bring about the desired $\Delta R = 0$ date was -3 deg. Therefore, a -2.45 deg correction was required with the first maneuver.

In summation, the nominal strategy consisted of a sequence of three maneuvers, executed on fixed revolutions, each of which simultaneously corrected and/or controlled the orbital parameters of interest in a predetermined, clearly defined

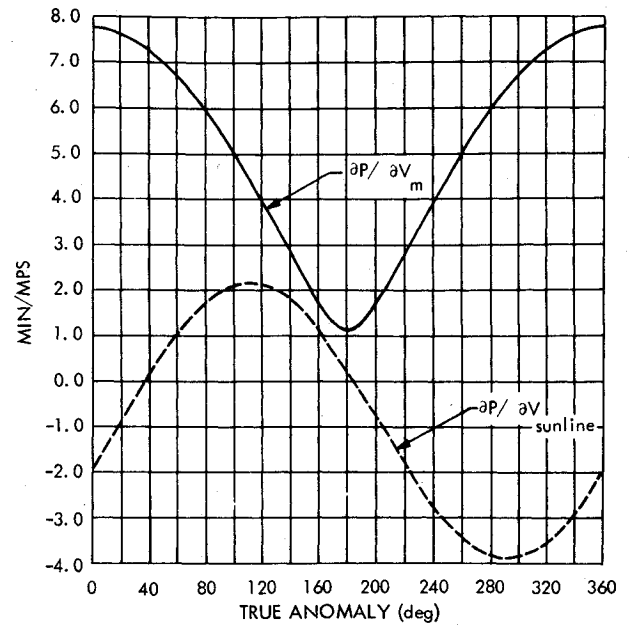


Fig. 9 Period (P) gradients.

fashion. The function of the first maneuver was to phase to the sync maneuver while simultaneously rotating the orbit. It was, in fact, responsible for most of the total orbit correction required. The role of the second maneuver was to synchronize with Phobos via a near apoapsis trim and to provide the final adjustment in orbit orientation. The last maneuver, also near apoapsis, would provide the "vernier" tune in timing required to meet the stringent period control requirements. Implicit in each maneuver definition was the requirement to compensate for the accumulation of any errors from previous maneuvers.

VIII. Maneuver Implementation

The design of the actual maneuver ΔV vector and time of ignition is conveniently solved in the flight plane velocity space (Fig. 8). Given the desired correction in each orbital element, the following equation is solved to determine a ΔV vector and the true anomaly at which to apply it.

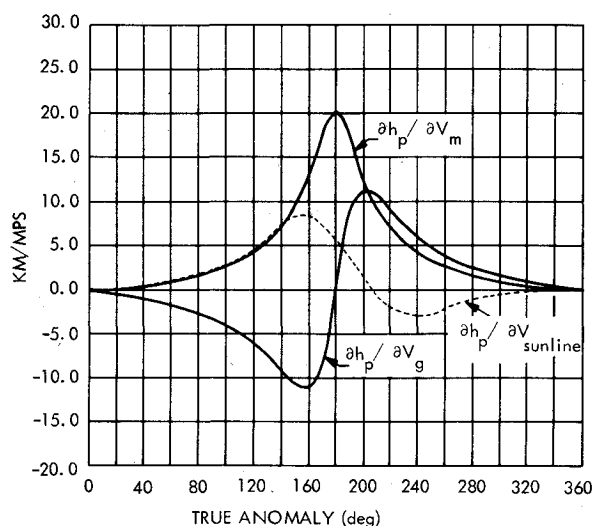
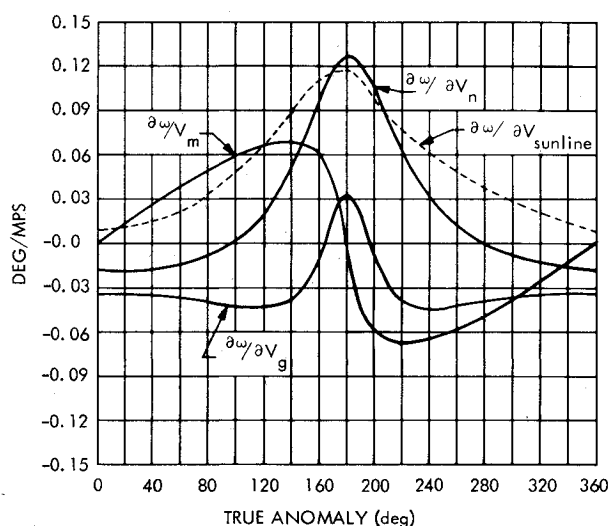
$$\begin{bmatrix} \Delta P \\ \Delta h_p \\ \Delta \omega \end{bmatrix} = \begin{bmatrix} \frac{\partial P}{\partial V_m} & 0 & 0 \\ \frac{\partial h_p}{\partial V_m} & 0 & \frac{\partial h_p}{\partial V_g} \\ \frac{\partial \omega}{\partial V_m} & \frac{\partial \omega}{\partial V_n} & \frac{\partial \omega}{\partial V_g} \end{bmatrix} \begin{bmatrix} \Delta V_m \\ \Delta V_n \\ \Delta V_g \end{bmatrix}$$

The maneuver sensitivity matrix is constructed as a function of true anomaly (η) from the gradient information in Figs. 9-11. The gradients were computed for an orbit with a 23 h period and a 1500 km h_p .

Since there are four controls and only three targets, one degree of freedom remained to minimize propellant, enhance Earth communications during the maneuver, and/or improve the final delivery accuracy. (Although the nominal Δh_p for all three maneuvers was zero, h_p was allowed to "float" slightly when improvement of navigation performance warranted an additional degree of freedom.) This methodology provided the means for evaluating a candidate maneuver's capability in attaining the designated target criteria. A suitable maneuver for the phase-rotation function was located at approximately 3 h after periapsis passage for 47 m/s. The requirements and actual performance for this maneuver are summarized in Table 1.

Table 1 Maneuver requirements and performances

Maneuver	Target	Control (99%)	Requirements	Achieved	Magnitude of error
First (phase)					
ΔP	- 1.581 h	± 58 s	Of no consequence to encounter control	- 1.594 h	47 s
Δh_p	- 10 km	± 5 km		- 14 km	4 km
$\Delta \omega$	- 2.45 deg	0.03 deg		- 2.43 deg	0.02 km
Second (sync)					
ΔP	- 2.43 min	± 5 s	± 5 s	- 2.41 min	2 s
Δh_p	0 km	± 1 km	± 5 km	+ 0.1 km	0.1 km
$\Delta \omega$	- 0.55 deg	± 0.01 deg	± 0.1 deg	- 0.54 deg	< 0.01 deg
Third (vernier)					
ΔP	- 1.35 min	± 2.5 s	± 3 s	- 1.35 min	< 0.1 s
Δh_p	+ 6 km	± 0.5 km	± 5 km	+ 6.3 km	0.3 km
$\Delta \omega$	+ 0.23 deg	± 0.1 deg	± 0.1 deg	+ 0.21 deg	0.02 deg

Fig. 10 Periapsis altitude (h_p) gradients.Fig. 11 Argument of periapsis (ω) gradients.

Previous to the execution of the phase maneuver, the development of the last maneuver was complicated by the ambiguity in the sign of the period correction. (The nominal period change was zero.) Originally, the intent was to perform the last two maneuvers nearly tangentially. Utilizing tangential maneuvers would produce an a priori guarantee on the final period control of ± 3 s (99%).

Subsequent to the phase maneuver execution, the sign of the final period correction would be determined. Inspection of

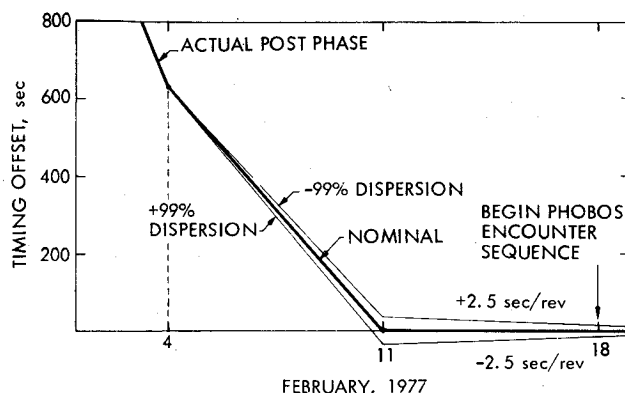


Fig. 12 Post phase maneuver timing diagram.

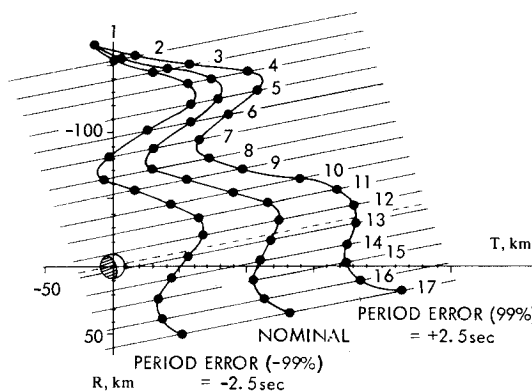


Fig. 13 Phobos encounter plane control.

the actual phasing results in Fig. 12 revealed that the final vernier period correction following all expected sync dispersions had to be negative (slope increasing). If the actual phasing period had produced a negative timing offset on February 4, the final period correction would have been positive. This timely knowledge led to a slight alteration in the nominal strategy which reduced the expected period errors to ± 2.5 s. This mapped into a 15 km reduction in the 99% dispersed encounter points on the $\Delta R = 0$ date.

The improved period control was obtained by executing the final maneuver in the spacecraft celestial cruise altitude, i.e., a "sunline" maneuver. During a sunline maneuver, the actual spacecraft orientation is better known and the pointing errors are noticeably reduced. Figures 9-11 show the capability for changing the parameters of interest, while leaving the spacecraft locked on its star and sun references. At 200 deg true anomaly the period and h_p sensitivities were ideal for a period decreasing maneuver. The period sensitivity was such that the ΔV would be just over the minimum duration burn

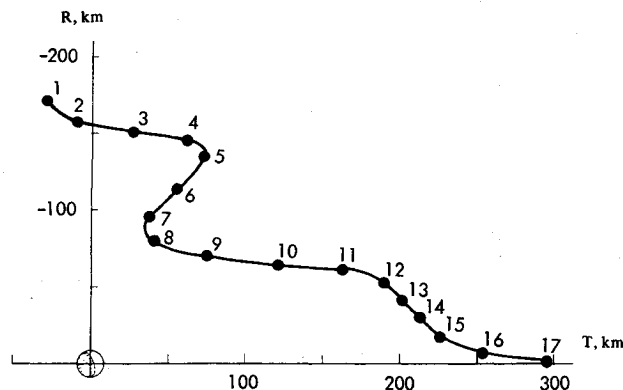


Fig. 14 Phobos encounter results.

allowable and the periapsis altitude sensitivity was nearly zero. Overall period control accuracy is influenced by the fixed ΔV magnitude error and pointing error. Directing the thrust away from the direction of the required correction reduces the effect of the former error and increases the effect of the latter error. Note that there is an optimal value of "misalignment" that minimizes the error. Because the thrust was directed approximately 70 deg from the period gradient, a significant reduction in the error variance was achieved. The sunline maneuver would also increase ω by 0.23 deg and move the $\Delta R = 0$ date to February 24. These changes were accepted in order to achieve the increased period control. The nominal encounter locus and expected dispersions for the sunline vernier trim are shown in Fig. 13.

A nominal sync maneuver was performed at 165 deg true anomaly for 5.5 mps and the sunline maneuver required 2.5 mps. The results are summarized in Table 1.

IX. Phobos Encounter Results

In Fig. 14 the actual flybys achieved are presented. All of the encounters were within 300 km with eleven of the encounters less than 175 km. The closest flyby was on February 20 at a distance of 88.9 km.

Early in the encounter mission it was apparent that the preflight value of $0.001 \text{ km}^3/\text{s}^2$ for the gravitational constant μ_p of Phobos was too high. Therefore, incorporation of an updated gravitational constant in the trajectory prediction used for the science sequence command loads was necessary in order to obtain pictures of Phobos. For the high-resolution picture sequences to be taken successfully, timing prediction accuracy to 1 or 2 s was required. The best estimate of μ_p determined from radio data by the Viking Satellite Orbit Determination Team was $0.00066 \text{ km}^3/\text{s}^2$ (Ref. 3). The perturbations to the V01 orbit period, assuming this value for μ_p , increased from 0 for encounter 1 to a maximum of 1.1 s at encounter 9, then slowly decreased to 0.5 s at encounter 17.

The encounters provided much scientific data. Over 125 pictures of Phobos were obtained at a resolution on the order of tens of meters. The imaging data were used to determine the volume and, consequently, the density of Phobos more accurately. Infrared coverage of Phobos was also obtained. These new data suggest a surface composition of Phobos which has ramifications on current theories on the origin and evolution of Phobos.⁴

X. Conclusions

A second opportunity for a series of Phobos encounters occurred in late May 1977. However, mission operations decided that a maneuver sequence would not be used to enhance this opportunity. Consequently, there was a single close encounter of approximately 300 km. Comparing this encounter to the February 1977 encounters shows the tremendous improvement in the quality of an encounter mission obtained from implementation of the trajectory and maneuver strategies presented in this paper.

An opportunity for a series of Deimos encounters occurred in October 1977. Using strategies similar to those used for the Phobos encounters, a series of three encounters was obtained. The closest encounter distance was targeted to approximately 30 km for the purpose of a Deimos mass determination.

These strategies are only valid for satellite encounters for which trajectory perturbations primarily affect orbital period. For such missions, the trajectory and maneuver strategies presented in this paper provide a basis for designing multiple close satellite encounters.

Acknowledgments

Several people have contributed to the strategy development and analysis presented in this paper. The authors especially acknowledge the efforts of R.T. Mitchell, D.L. Farless, C.E. Hildebrand, and R.P. Rudd (Langley Research Center).

This paper presents the results of one phase of research carried out at the Jet Propulsion Laboratory, California Institute of Technology, under Contract No. NAS 7-100, sponsored by NASA.

References

- ¹Masursky, H., et al., "Mariner 9 Television Reconnaissance of Mars and Its Satellites: Preliminary Results," *Science*, Vol. 175, 1972, pp. 294-305.
- ²Tolson, R.H., Blanchard, R.C., and Daniels, E.F., "Phobos and Deimos Encounter Experiment During the Viking Extended Mission," *Journal of Spacecraft and Rockets*, Vol. 13, Jan. 1976, pp. 19-25.
- ³Christensen, E.J., Born, G.H., Hildebrand, C.E., and Williams, B.G., "The Mass of Phobos From Viking Flybys," *Geophysical Research Letters*, Vol. 4, 1977, pp. 555-557.
- ⁴Tolson, R.H., et al., "Viking First Encounter of Phobos: Preliminary Results," *Science*, Vol. 199, 1978, pp. 61-64.